ORIGINAL PAPER

MMP7 damages the integrity of the renal tubule epithelium by activating MMP2/9 during ischemia–reperfusion injury

Qianchao Hu[1] · Jianan Lan[1] · Wenjin Liang[1] · Yiwen Chen[1] · Biao Chen[1] · Zhongzhong Liu[1] · Yan Xiong[1] · Zibiao Zhong[1] · Yanfeng Wang[1] · Qifa Ye[1,2]

Abstract

Renal ischemia–reperfusion (IR) injury is a common issue in urological surgery, and the renal tubules, particularly the proximal tubules, are extremely vulnerable to IR injury. In this work, we detected the differently expressed genes (DEGs) between normal rabbit kidneys and IR kidneys by RNA-sequencing, then identified that matrix metalloproteinase–7 (MMP7) played an important role in the progress of IR injury. Indeed, A time-dependent promotion of renal injury was detected in rabbit model, as demonstrated by the increased levels of MMP2/7/9, and the decreased of tight junction protein–1 (TJP1). Furtherly, similar results were confirmed in human renal proximal tubule epithelial (HK-2) cells model. Notably, downregulation of MMP7 affected the activity of MMP2/9 by suppressing expression of cleaved-MMP2/9 not the pro-MMP2/9 protein, which directly alleviated the degradation of TJP1 in HK-2 model. On the contrary, MMP7 had not been affected by inhibiting MMP2/9. In addition, coimmunoprecipitation assay showed that knockdown MMP7 restrained the interaction between MMP2/9 and TJP1. Collectively, this study suggested that MMP7 could serve as early biomarkers for renal tubular injury, and revealed that MMP7 could destroy the integrity of tubular epithelium through degrading TJP1 by activating MMP2/9.

Keywords Ischemia–reperfusion injury · Matrix metalloproteinase–7 · Kidney · Epithelium · Tight-junction components–1

Introduction

Ischemia–reperfusion (IR) injury to the kidney is a common consequence of urological surgery, especially during kidney transplantation (KT) (Ponticelli 2014; Saat et al. 2016), IR injury leads to tubular epithelial cell disfunction, furtherly contributes to acute kidney injury, delayed graft function, and acute and chronic rejection (Smith et al. 2019). Therefore, early intervention in this progress of renal IR injury may promote graft function and clinical outcomes in patients after KT. Unfortunately, there are no effective therapeutic target to prevent renal IR injury. To seek underlying interventional target, we detected the differently expressed genes (DEGs) between normal rabbit kidneys and IR (warm ischemia time for 35 min and reperfusion time for 1hour) injury kidneys by RNA-sequencing, and identified that matrix metalloproteinase–7 (MMP7) was most significantly overexpressed in IR kidneys.

MMP7, also called matrilysin, is a zinc- and calcium-dependent endopeptidase (Dunsmore et al. 1998), it can degrade a broad range of substrates, such as extracellular matrix (Ke et al. 2017) and cell–cell adhesion proteins (Shirahata et al. 2018; McGuire et al. 2003), to regulate cell migration and inflammation (Parks et al. 2004). Recently, plenty of studies suggested that urinary matrix metalloproteinase-7 (uMMP7) could be a biomarker to predict severe kidney diseases, such as acute kidney injury (AKI) (Fang et al. 2019), renal allograft inflammation and injury (Ho

✉ Zibiao Zhong
hizzb@whu.edu.cn

✉ Qifa Ye
yqf_china@163.com

1   Institute of Hepatobiliary Diseases, Transplant Center, Hubei Key Laboratory of Medical Technology on Transplantation, Zhongnan Hospital, Wuhan University, Wuhan 430071, China

2   Transplantation Medicine Engineering and Technology Research Center, National Health Commission, The 3rd Xiangya Hospital of Central South University, Changsha, China

et al. 2016), IgA Nephropathy (Yang et al. 2019) and kidney fibrosis (Zhou et al. 2017), and high level of uMMP7 are associated with poor in-hospital outcomes in patients after cardiac surgery (Yang et al. 2017). It is well confirmed that MMP7 is a downstream target gene of Wnt/β-catenin signaling pathway in proteinuric kidney diseases (Wang et al. 2011). The only one research studying the role of MMP7 in AKI revealed that MMP7 could degrade FasL and E-cadherin of renal tubule (Fu et al. 2019). However, the specific role and mechanism of MMP7 in damage of structure of renal tubule during IR injury is still incompletely understood.

Wang and Manole showed that overexpression of MMP7 damaged blood-nerve barrier by degrading tight junction proteins (TJPs) in peripheral nerve injury (Manole et al. 2015; Wang et al. 2018). TJP1 (also called ZO1) is the most common member of tight-junction components, distributing widely in endothelial and epithelial cells, and plays a key role in maintaining the integrity of the vessel and epithelia (Furuse and Tsukita 2006; Baker 2016; Farquhar and Palade 1963). Zhou X et al. revealed that oxidant injury caused a decrease in the expression of TJP1 in cultured kidney proximal tubular epithelial (HK-2) cells (Zhou et al. 2018). Moreover, the loss of TJP1 contributes to backleak in sustained allograft acute renal failure (Kwon et al. 1998). In addition, some studies have found that MMP2/9 can degrade TJP1 in vascular endothelium (Zhang et al. 2018; Wu et al. 2015). However, hitherto none study has revealed the effect of MMP7 on TJP1 and the interaction between MMP7 and MMP2/9 in renal IR injury.

In this study, we detected the expression of MMP7 both in rabbit renal IR injury model and HK-2 H/R model, and applied separately RNA interference and MMP2/9 inhibitor I to down regulate the MMP7 and MMP2/9. We found that knockdown of MMP7 can alleviate to degrade renal tubular epithelial TJP1 by decreasing the activated MMP2/9.

Materials and methods

Animal experimentation

This study was approved by *the Institutional Review Board/ Ethics Committee of Zhongnan Hospital of Wuhan University*. All animal experiments were carried out in accordance with *Experimental Animal Management Ordinance* (National Science and Technology Committee of China) and the *Guide for the Care and Use of Laboratory Animals* (National Institutes of Health, Bethesda, MD, USA).

Healthy male rabbits (12 weeks, 3.0 ± 0.3 kg) were obtained from Wan Qian Jia He Experimental Animal Culture Center (Wuhan, China). Before experiments, the animals were fasted for 12 h but had free access to water. After appropriate anesthesia, laparotomy was carried out. The left renal pedicles of rabbits were clamped for different warm ischemia time (WIT) (20, 35, 45, 60 and 90 min) by small vascular clamps, and body temperature was maintained at 38.5 ± 0.5 °C. Then, the clamps were loosened and the right kidney was excised (the right kidney was used as the sham group). After 24 h of reperfusion (when the WIT was fixed at 35 min, the reperfusion time was 1, 6, 12 or 24 h), kidney tissue and blood samples were collected for further test.

RNA-sequencing

Total RNA was extracted from samples. mRNA was enriched with Oligo (dT) magnetic beads. Fragmentation Buffer was added to the obtained mRNA to split it into short fragments. The latter were used to synthesize cDNA. cDNA chains were purified using a QIAquick™ PCR kit. We used EB buffer to repair them, and then recovered them by agarose gel electrophoresis. The target fragment was amplified by PCR. Single-end libraries were sequenced using a BGIseq-500 system (BGI Group, Guangzhou, China). Normalized gene expression was calculated using the reads per kilobase per million mapped reads method. A Student's *t*-test algorithm was used to identify DEGs between the different groups, and P-values were corrected using the Benjamini–Hochberg algorithm. DEGs defined from pairwise comparisons had to satisfy two selection criteria: fold-change > 2, and a corresponding $P < 0.05$.

Hematoxylin and eosin (HE) staining

Rabbit kidneys were fixed in 4% paraformaldehyde. Paraffin-embedded sections were stained with periodic acid-Schiff. Histology was carried out under light microscopy. Renal tubular necrosis was assessed by Paller scores. Ten randomly chosen, nonoverlapping fields per rabbit were evaluated.

Serum biochemistry

Blood samples were collected and centrifuged at 3000 rpm for 10 min and stored at -80 °C before analyses. Blood, urea, nitrogen and serum levels of Cr were analyzed by a Chemistry System analyzer (ADVIA 2400; Siemens, Tarrytown, NY, USA).

The terminal deoxynucleotidyl transferase dUTP nick end labeling (TUNEL) assay

The TUNEL assay was carried out with the One Step TUNEL Apoptosis Assay kit (C1086; Beyotime Biotechnology, Beijing, China) according to manufacturer instructions. Fluorescence images were captured using an inverted fluorescent microscope (TH4-200; Olympus, Tokyo,

Japan) at $\times 400$ magnification. The apoptosis rate was calculated according to the following formula: apoptosis rate = TUNEL-positive cells (n)/total cells (n) $\times 100\%$

RT-PCR

TRIzol™ Reagent (Thermo Fisher Scientific, Waltham, MA, USA) was used to extract the total RNA. Then, first-strand cDNA was synthesized using the Hifair® II 1st Strand cDNA Synthesis kit (Yeasen Biotech, Shanghai, China) according to manufacturer instructions. RT-PCR was carried out in StepOne Plus (Applied Biosystems, Foster City, CA, USA) using the Hifair III One Step RT-qPCR SYBR Green kit (Yeasen Biotech). The primer sets (forward and reverse, respectively) for qPCR were 5′-AGGAACGCATAA CAGGAC-3′ and 5′-GGATAGAGGATTAAAGTGAGGG-3′ for SOD1; 5′-TCGCTCTGAGGCACTACGG-3′ and 5′-TCA TTCTTGGCGTTCTCCGT-3′ for GPX1; 5′-TGGCTCTAA CAGTCCGCCTAG-3′ and 5′-AGTGCGACGTGGACATCC G-3′ for β-actin.

Western blotting

Western blotting was done as described previously (Zhong et al. 2016). We used several primary antibodies generated in rabbits: anti-MMP7 (1:1000; GeneTex, Inc., America), anti-MMP2 (1:1000; GeneTex, Inc., America), anti-MMP9 (1:1000; GeneTex, Inc., America), anti-TJP1 (1:1000; Wuhan Proteintech Group, China), and anti-β-actin (1:1000, Wuhan Proteintech Group). Bands were developed by an enhanced chemiluminescence (ECL) reagent. Protein expression was measured by densitometry analysis using ImageJ (National Institutes of Health).

Transmission electron microscopy (TEM)

First, 2.5% glutaraldehyde was added to kidney tissue. After fixation at 4 °C for 2 h, each kidney tissue was rinsed thrice with precooled phosphate-buffered saline (PBS) and dehydrated with acetone. Then, 1% osmic acid was added at room temperature for 2 h. Tissue was embedded in epoxy resin and dried, and ultrathin sections created after trimming. The ultrastructural changes and autophagosomes in each kidney were observed under a transmission electron microscope.

Culture and processing of cells

Human umbilical vein endothelial cells (HUVECs) and a human renal proximal tubule epithelial line (HK-2) were obtained from the Cell Bank of the Chinese Academy of Sciences (Beijing, China). HUVECs and HK-2 cells were cultured in Dulbecco's modified Eagle's medium (DMEM)

(high sugar) or DMEM/F12 medium + 10% fetal bovine serum (Biological Industries, America) at 37 °C in an atmosphere of 5% CO_2 and saturated humidity. When the cells had grown to 90% confluence, the supernatant was discarded. Adherent cells were washed twice with PBS, and serum-free DMEM (low sugar) was added. Then, cells were placed in a saturated tri-gas incubator at 37 °C in an atmosphere of 94% N_2, 5% CO_2 and 1% O_2 for 24 h to elicit hypoxia. After that, the supernatant was discarded, fresh total medium was added, and cells were re-oxygenated in a CO_2 incubator for 6 h.

RNA interference and gene transfection

siRNA oligonucleotides were synthesized by OBiO Technology (Shanghai, China). The siRNA gene sequences were three siRNA-MMP7 (Y8671: 5′-GCTCACTTCGAT GAGGATG-3′; Y8672: 5′-GCAGTCTAGGGATTAACT T-3′; Y8673: 5′-GGACATTCCTCTGATCCTA-3′) and one siRNA-NC (Y004: 5′-TTCTCCGAACGTGTCACG T-3′). The siRNA was loaded with a lentiviral vector and added to wells containing the cells and serum-free medium (no antibiotics). The cell culture plate was agitated gently and then incubated for 36 h at 37 °C in a CO_2 incubator. siRNA-NC or siRNA-MMP7 was transfected into cells and, after transfection, cells were exposed to hypoxic conditions for 24 h and reoxygenation for 6 h. The treatments were hypoxia/reoxygenation + Y004 (H/R + Y004) and hypoxia/reoxygenation + siRNA-MMP7 (H/R + Y8672).

Cell grouping

In the control group, HK-2 cells were incubated in normal conditions. In the H/R group, hypoxia was carried out for 24 h and reoxygenation for 6 h. In the H/R + Y004 group, HK-2 cells were incubated with siRNA-NC (Y004) in serum-free medium for 36 h and cultured further under the same conditions as described in the H/R group. In the H/R + Y8672 group, HK-2 cells were cultured with lentivirus carrying the siRNA of MMP7 (Y8672) in serum-free medium for 36 h and then cultured under the same conditions as described in the H/R group. In the H/R + MMP2/9 inhibitor I group, hypoxia was undertaken for 24 h with 60 μM of MMP2/9 inhibitor I (ab145190; Abcam, Cambridge, UK) and then reoxygenation for 6 h. In the 1 mM group, HK-2 cells were cultured with 1 mM H_2O_2 for 6 h. In the 1 mM + Y8672 group HK-2 cells were cultured with lentivirus carrying the siRNA of MMP7 (Y8672) in serum-free medium for 36 h and then cultured under the same conditions as described in the 1 mM group.

Reactive oxygen species (ROS) detection

Intracellular ROS levels were measured using a ROS fluorescence probe: 2′,7′-Dichlorodihydrofluorescein diacetate (DCFH-DA). After treatment in each group individually, cells were incubated with serum-free medium and DCFH-DA (10 μM) at 37 °C for 25 min. Then, cells were washed gently thrice with PBS. Immediately, fluorescence images were obtained with a fluorescence microscope (Olympus, Japan).

Immunofluorescence

After treatment in each group individually, the cell medium was removed and washed thrice with PBS, and then fixed in 4% paraformaldehyde for 20 min. After permeabilization in 0.3% Triton X-100 for 10 min, blockade with 5% bovine serum albumin for 30 min at room temperature was carried out. Then, cells were incubated with the anti-TJP1 in 5% bovine serum albumin overnight at 4 °C. This was followed by incubation with a mixture of CoraLite 488-conjugated Affinipure goat anti-rabbit IgG (H+L) and CoraLite 594-conjugated goat anti-mouse IgG (H+L) (Wuhan Proteintech Group) for 1 h at room temperature in the dark. Then, cell nuclei were stained with 4′,6-Diamidino-2-phenylindole dihydrochloride in PBS (10 μg/ml) for 10 min. Images were acquired using a fluorescence microscope (Olympus).

Coimmunoprecipitation (CO-IP) assay

The protein concentration of HK-2 cell extracts was determined using a Bicinchoninic Acid Protein Concentration Assay kit (Wuhan Servicebio Biotechnology, Hubei, China), and 0.5 mg of total protein lysates were used for coimmunoprecipitation. Lysates were incubated with 3 mg antibody or rabbit polyclonal IgG control antibody (Wuhan Proteintech Group). Samples were incubated with slight agitation overnight at 4 °C. Next, 25 μl of Protein A/G Plus-Agarose (Thermo Fisher Scientific) was added to samples and rotation continued for 10 h. The resulting complexes were washed, denatured, and eluted according to manufacturer instructions. Western blotting was done, and immune-reactive bands were visualized using an ECL method (ECL kit; Wuhan Servicebio Biotechnology). Quantification of protein bands was carried by using ImageJ.

Statistical analyses

Results are presented are the mean ± SD. Correlations were evaluated by Pearson's correlation. Differences between groups were analyzed using the Student's t-test, one-way ANOVA, Mann–Whitney U-test or χ^2 test.

Statistical analyses were undertaken using SPSS 17.0 (IBM, Armonk, NY, USA). $P < 0.05$ was considered significant. Prism 5.0 (GraphPad, San Diego, CA, USA) was used to prepare graphs.

Results

Effect of warm ischemia and reperfusion on injury to rabbit kidneys

We established a model of renal IR injury in rabbits to study the effect of the warm ischemia time (WIT) and reperfusion time. Under a fixed reperfusion time (24 h), rabbit kidneys were treated with different WIT. The creatinine (Cr) concentration was highest at WIT 90 min. Also, ΔCr ($\Delta Cr = Cr$ (postoperative) – Cr (preoperative)) at WIT 35 min increased significantly compared with that of WIT 20 min ($P < 0.0001$, n = 6), and was close to that of WIT 45–60 min (Fig. 1c). HE staining showed that, with prolongation of the WIT, the Paller score of the kidneys increased gradually (Fig. 1a, b). The damage wrought by WIT 90 min was irreversible: ≥ 90% of renal tubules necrosed. The damage caused by a WIT of 35 min caused an intermediate effect: 30–40% of renal tubules necrosed (Fig. 1a, b). These data suggested that WIT 35 min could cause partial injury to the kidney. Hence, we employed WIT 35 min to observe renal damage at different reperfusion times.

Under a fixed WIT (35 min), rabbit kidneys underwent reperfusion for different times. The Cr concentration began to increase from 1 h after reperfusion (Fig. 2c). The TUNEL assay demonstrated that, with prolongation of the reperfusion time, the apoptotic level in kidney tissue increased gradually (Fig. 2a, b), but there was no significant difference between the sham group and 1 h after reperfusion ($P = 0.0571$, Fig. 2b). Expression of oxidative stress-related enzymes was measured by RT-PCR. Superoxide dismutase (SOD)-1 expression reached a peak 6 h after reperfusion and then decreased, and glutathione peroxidase (GPX)-1 expression decreased gradually with time (Fig. 2d, e). These data suggested that the level of oxidative stress increased with time, but there was no significant difference between the sham group and 1 h after reperfusion.

These results suggested that, when the time of ischemia–reperfusion was 35 min^{-1} h, some "potential molecules" had started to change, which subsequently caused renal damage with prolongation of reperfusion time, even though there was no morphological change or apoptosis in kidneys. Therefore, further tests needed to be done to search for these "potential molecules".
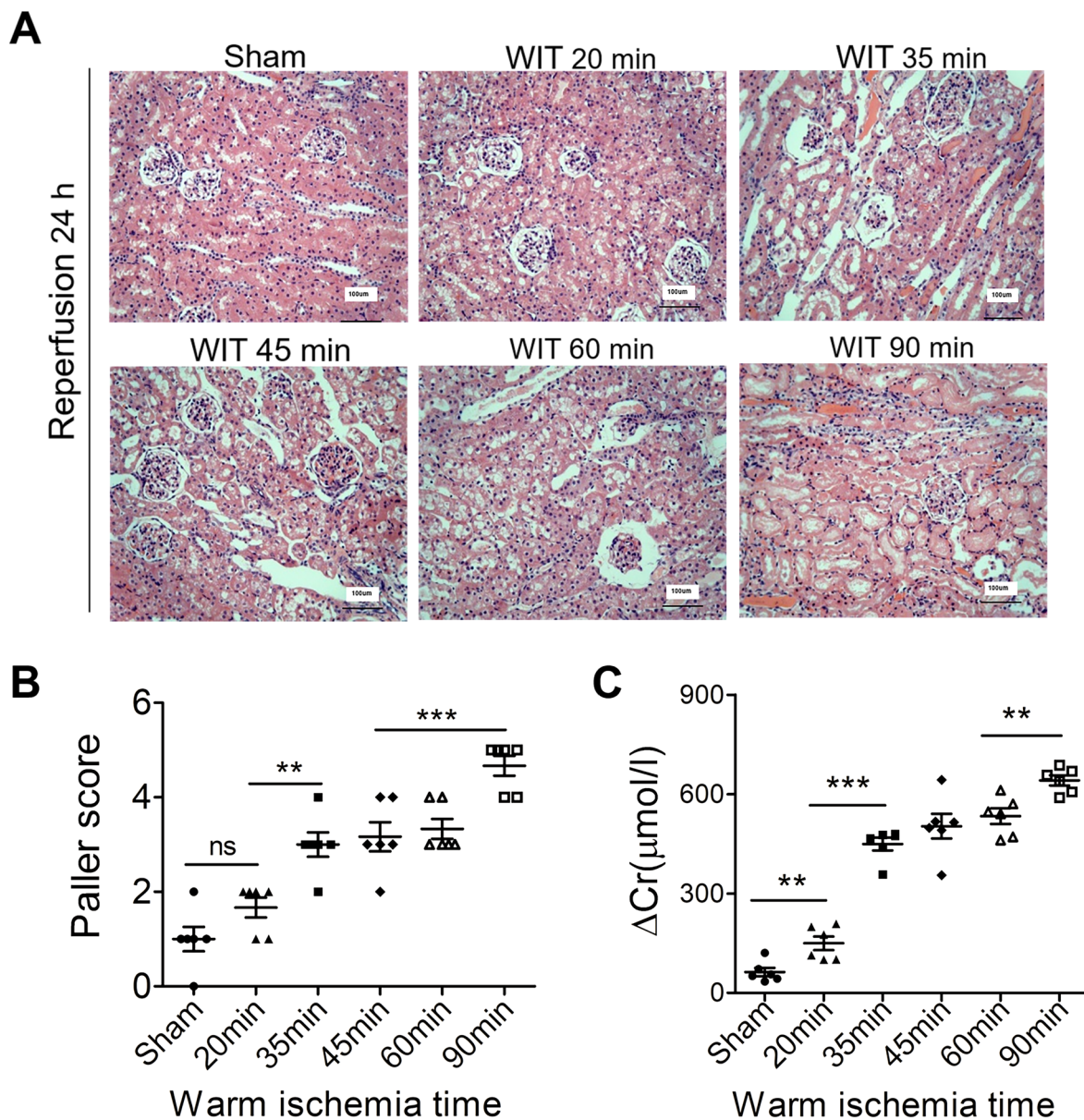
Fig. 1 Effect of warm ischemia on rabbit kidney injury. **a** H&E staining was used to detect the histology of renal injury (×200 magnification). **b** Paller scores in different groups calculated from H&E staining indicate that renal damage after WIT 35 min was more serious than WIT 20 min (**$P=0.0025$, n=6/each), close to that achieved with a WIT of 45–60 min, and less than that with a WIT of 90 min ($P=0.0005$, n=6/each). **c** ΔCr of WIT 35 min was significantly higher than that of WIT 20 min ($P<0.0001$, n=6/each), and reached to the Cr-raised plateau

Differentially expressed genes (DEGs) between sham kidneys and IR kidneys

We used RNA-seq to probe the "potential molecules" in IR (35 min^{-1} h) kidneys. There were 201 DEGs between the two groups (sham vs. IR): 110 upregulated genes and 91 downregulated genes. Among the top-20 DEGs, MMP7 was the most significant gene (Fig. 3a). In the family of MMPs, only MMP7 was overexpressed significantly in IR kidneys according to the heatmaps (Fig. 3b). Plots (volcanic, M/A, scatter) revealed that MMP7 was significantly overexpressed in IR kidneys (Fig. 3c–e). Western blotting also demonstrated that expression of MMP7 protein in IR was significantly higher than that in the sham group ($P<0.05$, Fig. 3g, h). A
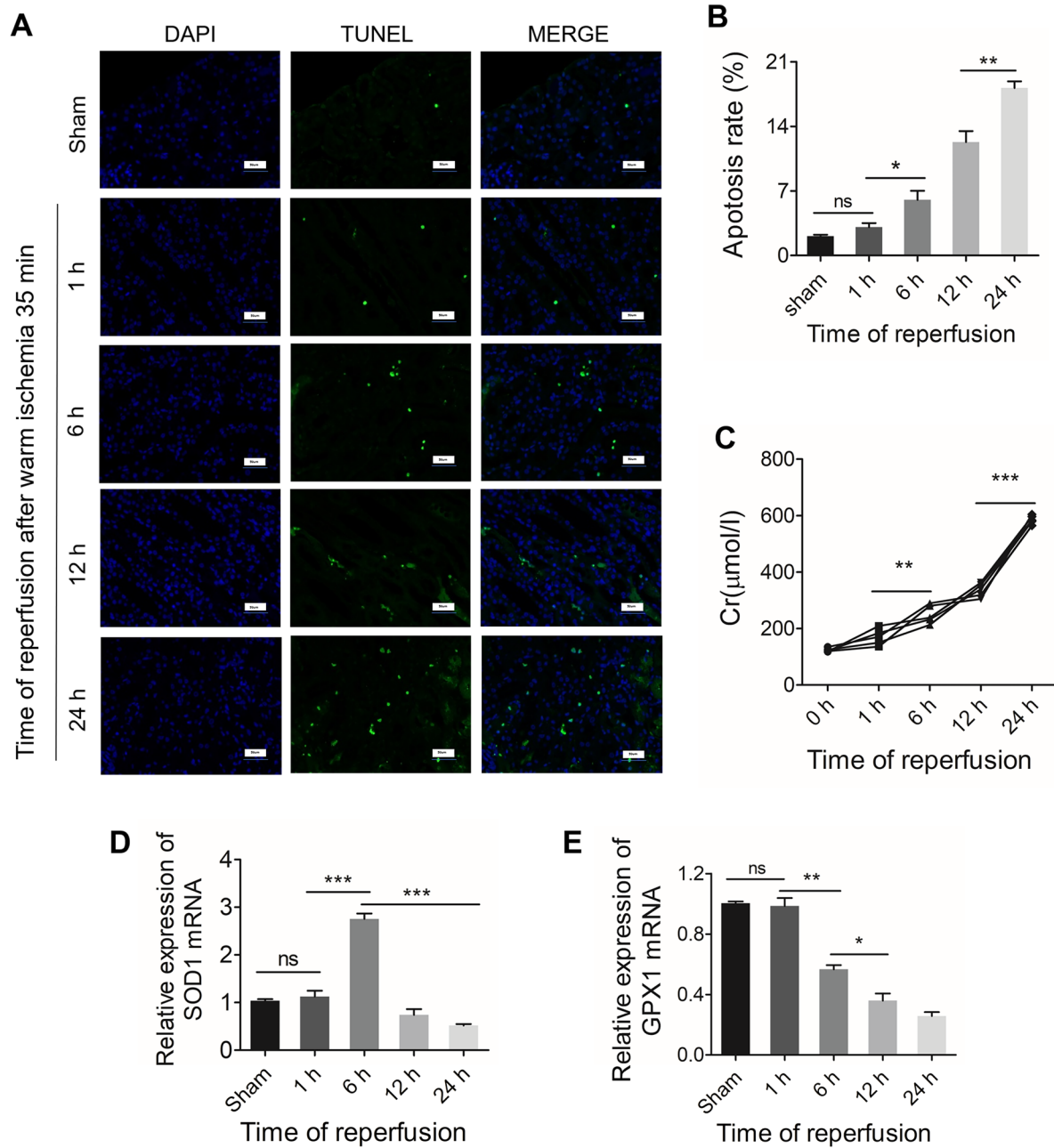
Fig. 2 Effect of reperfusion on rabbit kidney injury. **a** TUNEL assay showed apoptotic cells in kidney tissue after different reperfusion time (×400 magnification). **b** The apoptosis rate calculated from the TUNEL assay (*P = 0.0338, **P = 0.0056, n = 5/each). **c** The level of serum Cr increased with reperfusion time within 24 h (**P = 0.0032, ***P < 0.0001, n = 5/each). **d** and **e** The level of oxidative stress was indicated by expression of SOD1 mRNA and GPX1 mRNA. **d** SOD1 mRNA (*P = 0.0156, ***P < 0.001, n = 5/each), **e** GPX1 mRNA (*P = 0.0185, **P = 0.0017, n = 5/each)

simplified network obtained by *STRING* analysis showed that MMP7 may interact with MMP2/9 and TJP1 (Fig. 3f).

These results suggested that MMP7 had started to be expressed in large quantities in the early stage of renal IR.

Hence, MMP7 could be used as biomarkers of renal IR injury. Our data also suggested that MMP7 could be associated with MMP2/9 and TJP1 in renal IR injury.
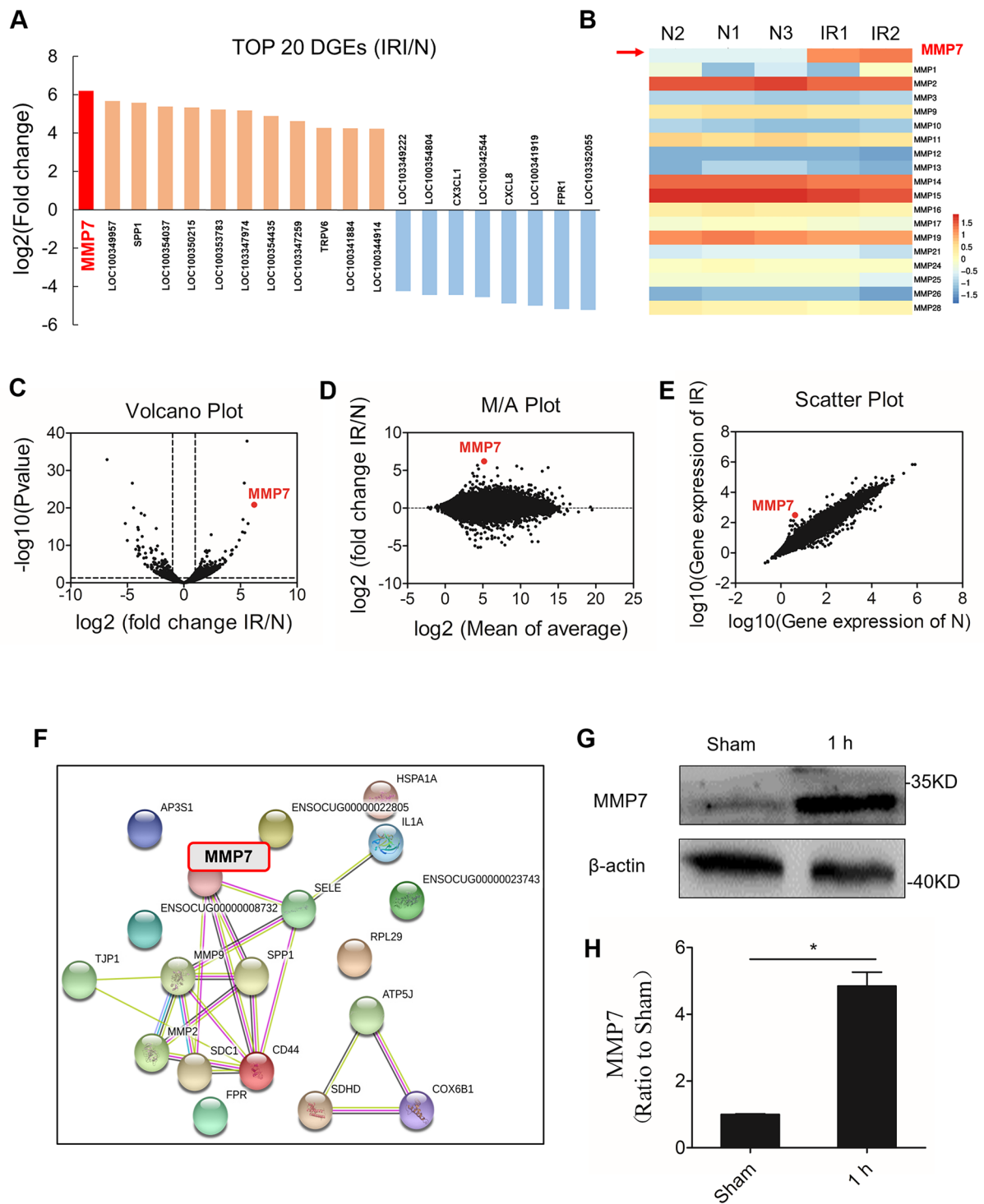
Fig. 3 MMP7 were highly expressed in the early stage of renal IR compared with sham. **a** Top 20 DEGs are displayed in a histogram. **b** Heatmap showing the family members of MMPs genes detected from rabbit kidneys. **c–e** Volcano plot, M/A plot and scatter plot showing the distribution of DEGs. **f** A simplified network obtained by STRING analyses. **g** and **h** The expression of MMP7 detected by western blotting (*P < 0.05, n = 4/each)
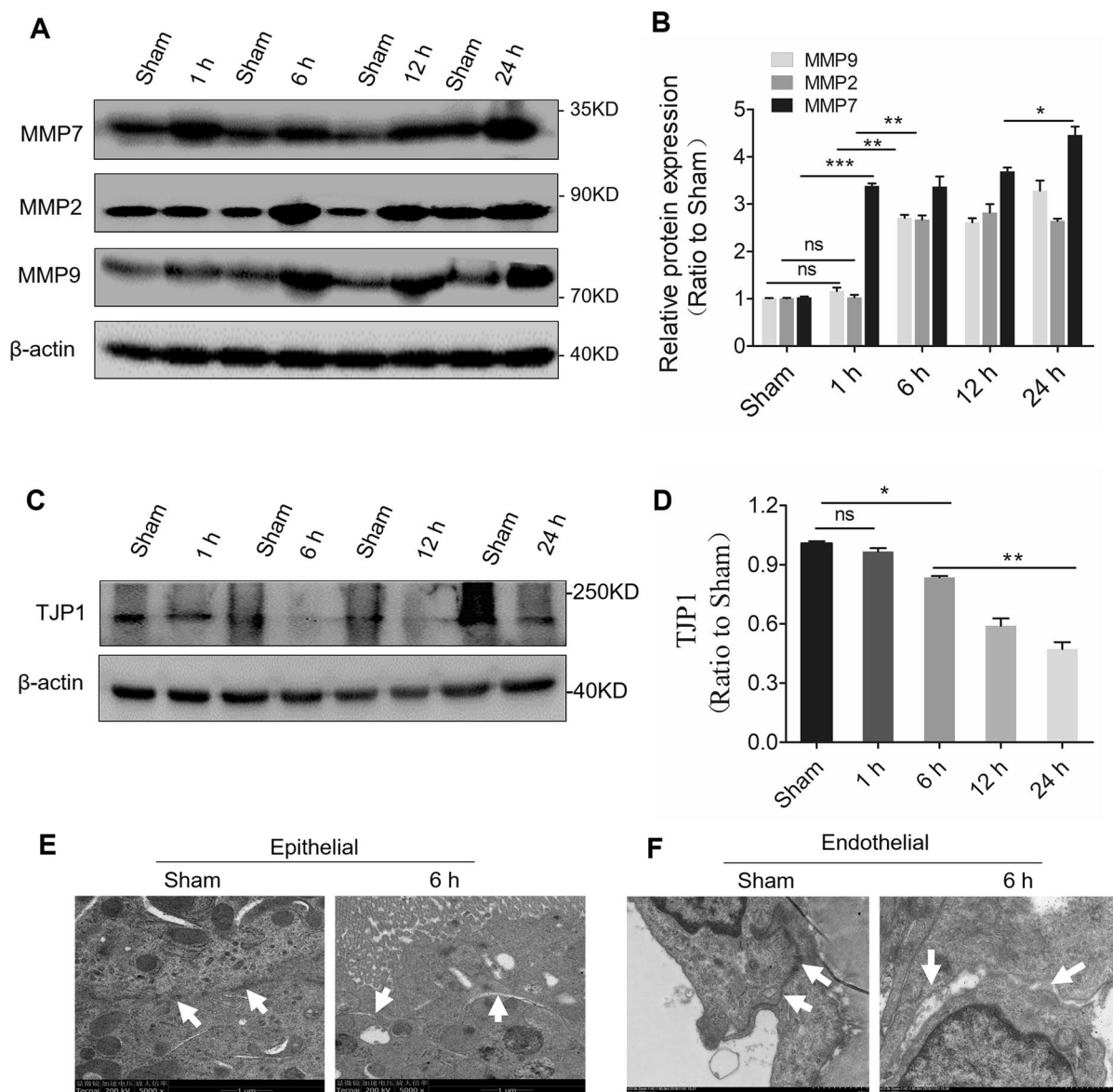
Fig. 4 Expression of MMPs increased with prolongation of the reperfusion time, whereas the degradation of TJP1 increased. **a** Western blotting detected the expression of MMP2/7/9. **b** The expression of MMP2/7/9 are displayed in a histogram (*P < 0.05, **P < 0.01, ***P < 0.001, n = 4/each). **c** Western blotting showed that expression of TJP1. **d** The expression of TJP1 are displayed in a histogram (*P < 0.05, n = 4/each). **e** and **f** TEM showed the ultrastructure of the tubular epithelium (**e**) and arterial endothelium (**f**) (× 5000 magnification, white arrows indicated that the cellular gap broadened in IR compared with the sham group)
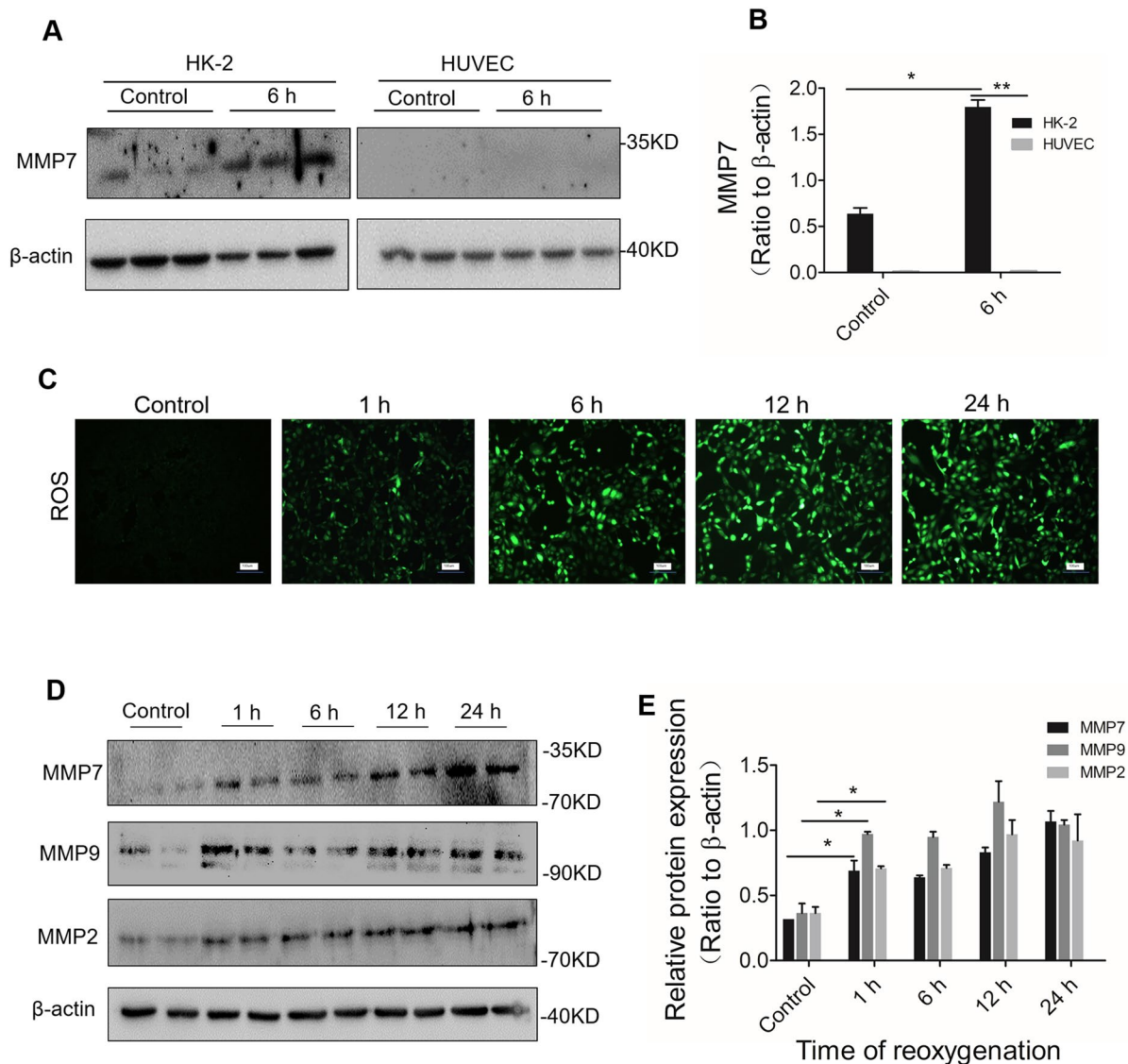
Expression of MMPs increased with prolongation of the reperfusion time, whereas the degradation of TJP1 increased

The change in expression trends of MMP2/7/9 and TJP1 in IR kidneys was studied. Western blotting showed that expression of MMP2/7/9 increased gradually with prolongation of the reperfusion time. One hour after reperfusion, only expression of MMP7 increased, whereas MMP2/9 expression did not. These data suggested that MMP7 was more sensitive to IR injury than MMP2/9.

MMP2/9 expression began to increase after 6 h of reperfusion (Fig. 4a, b). Expression of TJP1 in kidney tissue (as detected by western blotting) decreased gradually with prolongation of the reperfusion time (Fig. 4c, d). TEM showed that the intercellular gap between renal epithelial cells widened (Fig. 4e) and renal arterial endothelial cells began to exfoliate after 6 h of reperfusion (Fig. 4f).

These results suggested that expression of MMP7, MMP2/9 and TJP1 was time-dependent upon reperfusion. Expression of MMP7 changed earlier than that of other

Fig. 5 In HK-2 cells, after 24 h of hypoxia, expression of MMPs and ROS increased with the time of reoxygenation. **a-b** In HUVECs and HK-2 cells treated with H/R, expression of MMP7 was detected by western blotting (*P = 0.0383, **P < 0.005, n = 3/each). **c** ROS pro- duction increased with the reoxygenation time in HK-2 cells (×200 magnification). **d** and **e** Western blotting showed the expression of MMP2/7/9 in HK-2 cells (*P < 0.05, n ≥ 3/each)

molecules, and augmentation of MMP2/7/9 expression was accompanied with decreased expression of TJP1.

In HK-2 cells, after 24 h of hypoxia, expression of MMPs and intracellular ROS increased with prolongation of reoxygenation time

To identify the expression site of MMP7, we carried out hypoxia for 24 h and reoxygenation for 6 h in HUVECs and HK-2 cells. The expression of MMP7 was detected by western blotting. In HUVECs, expression of MMP7 was very little both in control group and hypoxia/reoxygena- tion (H/R) group. In HK-2 cells, expression of MMP7 in H/R group was higher than that in control group (Fig. 5a, b). Therefore, subsequent experiments were carried out in HK-2 cells. ROS measurement showed that, with prolon- gation of reoxygenation time, ROS production increased gradually (Fig. 5c). Western blotting showed that expres- sion of MMP2/7/9 increased gradually with prolongation of reoxygenation time (Fig. 4f, g).

However, compared with the results from the in vivo study, expression of MMP2/9 and MMP7 increased simultaneously in the H/R model in HK-2 cells. Besides, there was no significant difference in oxidative-stress response between the IR 1 h group and sham group in the rabbit model (Fig. 2d, e), but there was a significant difference in ROS production between the H/R 1 h group and control group in the HK-2 cells model (Fig. 5c). Therefore, we speculated that MMP2/9 expression may have been regulated by ROS production.
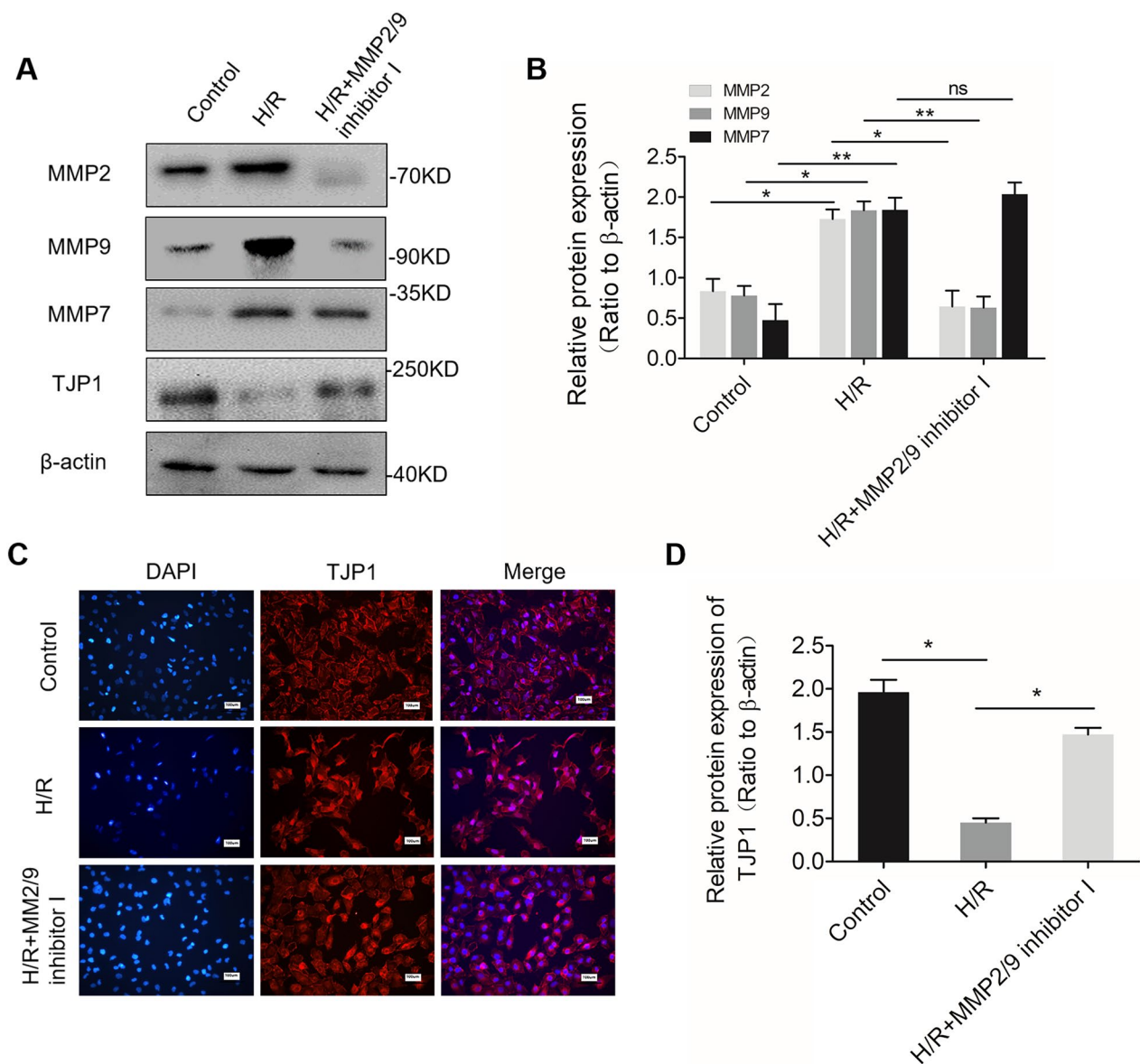
Downregulation of MMP7 expression did not affect MMP2/9 expression, but reduced the damage to TJP1. Downregulation of MMP2/9 expression also reduced the degradation of TJP1 by MMP2/9 inhibitor I

To clarify the relationship between MMP7 and other molecules, three plasmids of siRNA–MMP7 (Y8671, Y8672, Y8673) and one siRNA–NC (Y004) were constructed. The transfection efficiency was ≥ 99% using lentiviruses (Supplementary Fig. 1A). Western blotting showed that Y8672
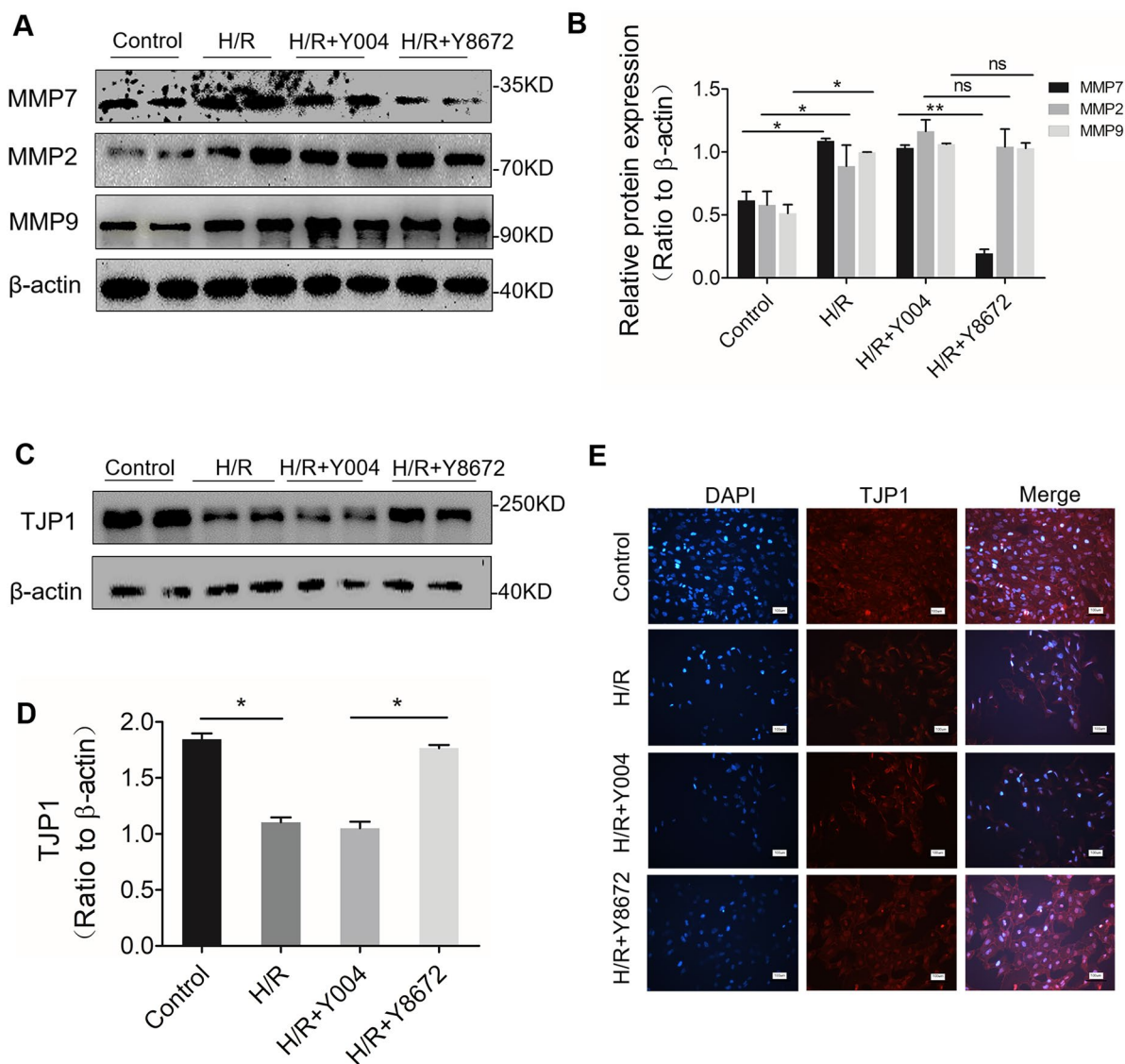
Fig. 6 Knockdown of MMP7 expression did not affect expression of MMP2/9, but reduced the damage to TJP1 in H/R. **a** and **b** Western blotting showed that down-regulation of MMP7 expression could reduce MMP7 expression, but could not affect expression of MMP9 in H/R (*P < 0.05, **P < 0.005, n ≥ 3/each). **c** and **d** Western blotting showed that expression of TJP1 in the H/R + Y8672 group was higher than that in the H/R + Y004 group (*P < 0.05, n ≥ 3/each). **e** Immunofluorescence showed that after down-regulating expression of MMP7, the degradation of TJP1 was reduced in H/R observed under a fluorescence microscope (×200 magnification)

Fig. 7 Down-regulation of expression of MMP2/9 did not affect expression of MMP7, but reduced the damage to TJP1 in H/R. **a** and **b** Western blotting showed that down-regulation of MMP2/9 expression could reduce MMP2/9 expression, but could not affect expression of MMP7 in H/R (*P < 0.05, **P < 0.01, n ≥ 3/each). **c** Immunofluorescence showed that after down-regulating expression of MMP2/9, the degradation of TJP1 was reduced in H/R observed under a fluorescence microscope (×200 magnification). **d** MMP2/9 inhibitor I could reduce the degradation of TJP1 (*P < 0.05, n ≥ 3/ each)

could better knockdown MMP7 expression than the other agents tested (Supplementary Fig. B-C). After that, Y8672 was used to knockdown MMP7 expression.

MMP7 expression was decreased significantly by Y8672 (P < 0.001), but expression of MMP2/9 and SPP1 was not affected in the IR + Y8672 group (Fig. 6a, b). However, immunofluorescence studies showed that down-regulation of MMP7 expression could alleviate the shedding of TJP1 (Fig. 6e). Western blotting also demonstrated that expression of TJP1 in the IR + Y8672 group was significantly higher

than that in the IR + Y004 group (P < 0.05, Fig. 6c, d). These data suggested that downregulation of MMP7 expression could alleviate the shedding of TJP1.

Furthermore, we employed MMP2/9 inhibitor I to down-regulate MMP2/9 expression, Western blotting showed that if MMP2/9 expression was reduced, H/R caused the degradation of TJP1 in HK-2 cells to be reduced too, even though MMP7 expression was not affected (Fig. 7a, b, d). Immunofluorescence studies also showed that down-regulation of MMP2/9 expression could alleviate the shedding of TJP1 (Fig. 7c).
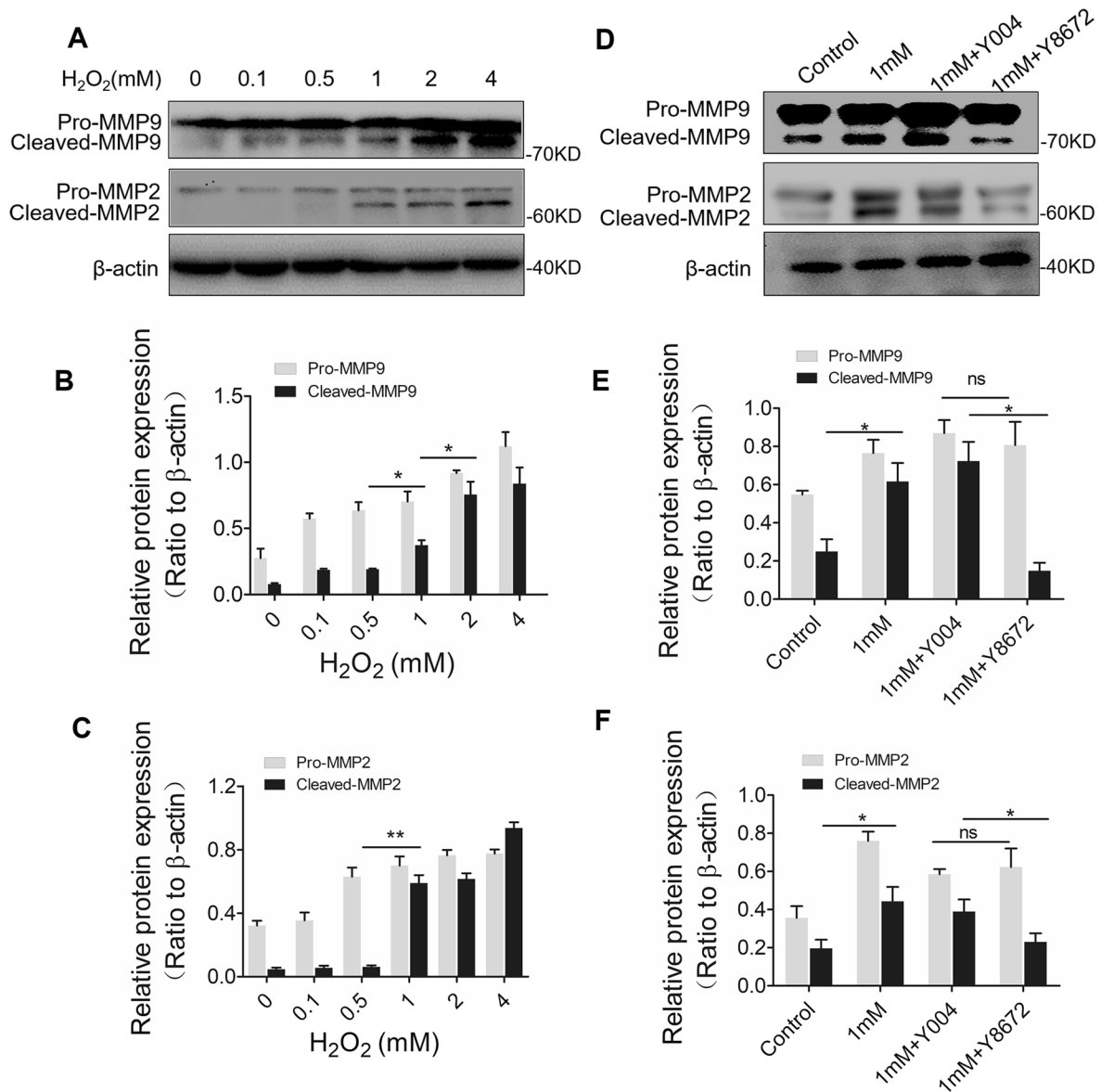
Fig. 8 In HK-2 cells, expression of pro-MMP2/9 and cleaved-MMP2/9 increased with increasing H_2O_2 concentration, and expression of cleaved-MMP2/9 decreased after knockdown of MMP7 expression. **a–c** Western blotting showed that with increasing H_2O_2 concentration, expression of pro-MMP9 and cleavd-MMP9 (**b**), pro-MMP2 and cleaved-MMP2/9 (**C**) in cell culture medium increased gradually (*P < 0.05, **P < 0.01, n ≥ 3/each). **d–f** After knockdown of MMP7 expression, cleaved-MMP2/9 expression in cell culture medium treated with 1 mM of H_2O_2 was reduced, whereas expression of pro-MMP2/9 was unchanged (*P < 0.05, n ≥ 3/each)

These results suggested that, if MMP2/9 expression was downregulated by MMP2/9 inhibitor I in the H/R model, without affecting MMP7 expression, then degradation of TJP1 was alleviated. Meanwhile, if MMP7 expression was downregulated, without affecting MMP2/9 expression, degradation of TJP1 was also alleviated. We speculated that MMP7 could degrade TJP1 in the presence of MMP2/9. However, the specific relationship between MMP7 and MMP2/9 had to be studied further.

In HK-2 cells, expression of pro-MMP2/9 and cleaved-MMP2/9 increased with increasing H_2O_2 concentration, but expression of cleaved-MMP2/9 decreased after knockdown of MMP7 expression

To clarify the effect of ROS on MMP2/9 expression, we carried out oxidative stress model. Western blotting showed that expression of pro-MMP2/9 and cleaved-MMP2/9 increased with increasing H_2O_2 concentration
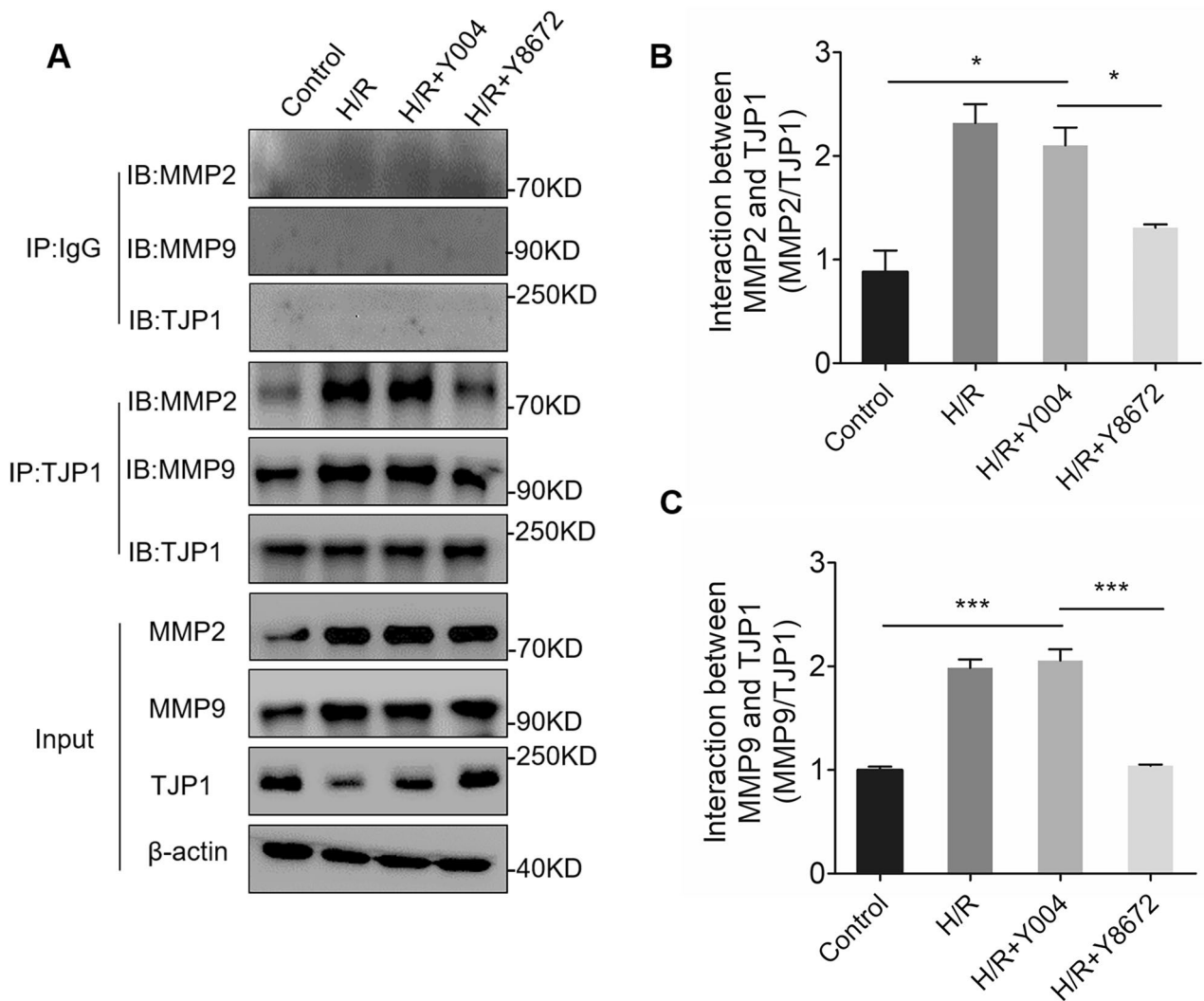
Fig. 9 Downregulation of MMP7 expression could reduce the combination of MMP2/9 with TJP1. **a–c** CO-IP showed that downregulation MMP7 could reduce the combination of MMP2/9 with TJP1

significantly, whereas MMP9 expression was not affected (*P < 0.05, ***P < 0.001, n = 3/each)

(Fig. 8a–c). However, after knocked down MMP7 expression, western blotting showed that, although pro-MMP2/9 expression did not change, expression of cleaved-MMP2/9 decreased significantly (P < 0.05) (Fig. 8d–f). These results suggested that MMP7 could activate pro-MMP2/9 to cleaved-MMP2/9.

These results suggested that MMP2/9 expression was regulated by the level of ROS. MMP7 did not affect MMP2/9 expression, but could enhance cleaved-MMP2/9 expression. Therefore, taken together with previous results, we concluded that MMP7 could degrade TJP1 by activating MMP2/9 in HK-2 cells.

Downregulation of MMP7 expression could reduce the combination of MMP2/9 with TJP1

To further confirm the conclusion stated above, we conducted CO-IP experiments to explore the combination of MMP2/9 with TJP1 after down-regulating MMP7 expression. Results showed that downregulation of MMP7 expression could not reduce MMP2/9 expression, but that the combination of MMP2/9 with TJP1 was reduced significantly (Fig. 9a–c), which suggested that MMP7 was helpful in activating MMP2/9 to combine with TJP1 and degrade it. These results confirmed our conclusion that

MMP7 could degrade TJP1 of HK-2 cells by activating MMP2/9.

Discussion

In this study, we carried out RNA-seq to probe the underlying mechanism of renal IR, and identified that MMP7 significantly overexpressed in rabbit IR kidneys (ischemia for 35 min and reperfusion for 1hour). Subsequently, knockdown of MMP7 expression alleviated the degradation of TJP1 by inhibiting expression of cleaved-MMP2/9 in HK-2 model. These results provide strong evidence that MMP7 contributes to renal tubular TJP1 degradation during kidney IR injury and suggest that pharmacological targeting of MMP7 might be prevent integrity of renal tubule epithelium from destroying.

It is well known that proximal tubular epithelium is especially subject to I/R injury, due to the high energy consumption (Tirapelli et al. 2009; Gewin 2018). Numerous studies showed that tubular epithelium detached from the basement membrane in the pathophysiology of acute renal failure (Goligorsky et al. 1993). However, not all tubular cells shedding from the basement membrane are necrotic or apoptotic death of cells, some are still viable (Racusen and Solez 1991). Moreover, junctional instability of the tubular epithelium furtherly promotes kidney injury (Berzal et al. 2015). Therefore, it is necessary to verify the underlying mechanism of exfoliation of renal tubular epithelium in IR injury.

In this study, TEM showed that reperfusion 6 h after WIT 35 min, renal arterial endothelial cells began to exfoliate and the intercellular gap between renal epithelial cells widened (Fig. 4e, f), and western blotting detected that the expression of TJP1 significantly decreased in IR kidney (Fig. 4c, d). TJP1 is one of major components of tight junctions in the proximal tubule, and plays an important role in maintaining the epithelium polarity and barrier integrity of renal tubule (Yu and Alan 2015). Loss of TJP1 causes the disfunction of absorption/excretion of fluid and solutes (Prozialeck and Edwards 2007). However, it is still uncertain that the mechanism of degradation of TJP1 in renal IR injury.

To find the trigger, RNA-seq were used to detect the DEGs in IR kidneys, MMP7 expression increased significantly in kidneys exposed to IR injury (Fig. 3). As mentioned in the introduction, MMP7 can regulate the expression of TJP1 in blood-nerve barrier (Wang et al. 2018). Additionally, MMP7 synthetizing from renal epithelium can lead to nephrin depletion and impaired glomerular permeability in proteinuric chronic kidney disease(Tan et al. 2019). Whether MMP7 can lead to TJP1 depletion in tubular epithelium is unknown.

In our study, downregulation of MMP7 decreased the degradation of TJP1 in HK-2 H/R model (Fig. 6c–e). To our known, IR injury has been verified to degrade the TJPs in blood–brain barrier due to MMP2/9 overexpression(Zhang et al. 2018). So, we also used the MMP2/9 inhibitor I (Tamura et al. 1998)(cannot inhibit MMP7) to down regulation of MMP2/9, results suggested that after treated with MMP2/9 inhibitor I, the degradation of TJP1 in HK-2 decreased as well (Fig. 7). However, we found that MMP2/9 expression did not increase in renal IR (WIT 35 min/reperfusion 1 h) group compared with sham group according to RNA-seq (Fig. 3b). Therefore, the relationship between MMP7 and MMP2/9 in degradation of TJP1 in IR injury is not clear. Western blotting showed that expression of MMP7 preceded MMP2/9 in rabbit renal IR injury model (Fig. 4a, b). Meanwhile, knockdown MMP7 abated the activation of MMP2/9 in HK-2 oxidative stress model (Fig. 8d–f). CO-IP also showed that knockdown of MMP7 expression reduced the binding of MMP2/9 to TJP1, and prevented TJP1 degradation (Fig. 9). Therefore, from those results, we can deduce that overexpression of MMP7 leads to degrade TJP1 of renal tubular epithelium by activating MMP2/9 in IR injury.

It should be emphasized that MMP7 can reduce renal tubular apoptosis by cutting FasL and E-cadherin (Fu et al. 2019). This seems to contradict our conclusion. In fact, our study focuses on the effect of MMP7 on TJP1 of renal tubule, not on the effect of MMP7 on apoptosis, moreover, degradation of TJP1 doesn't mean cell apoptosis. Previous studies have shown that not all tubular cells shedding from the basement membrane are necrotic or apoptotic death of cells, some are still viable(Racusen and Solez 1991). Therefore, it is indiscreet to declare that our research is contradictory to theirs.

In conclusion, expression of MMP7 is increased in renal IR injury. MMP7 can damage TJP1 of renal tubular epithelial cells by activating MMP2/9. Therefore, our study provides a new theoretical basis for improving renal IR injury.

Compliance with ethical standards

References

Baker OJ (2016) Current trends in salivary gland tight junctions. Tissue Barriers 4(3):e1162348. https://doi.org/10.1080/21688370.2016.1162348

Berzal S, González-Guerrero C, Rayego-Mateos S, Ucero Á, Ocaña-Salceda C, Egido J, Ortiz A, Ruiz-Ortega M, Ramos AM (2015) TNF-related weak inducer of apoptosis (TWEAK) regulates junctional proteins in tubular epithelial cells via canonical NF-KB pathway and ERK activation. J Cell Physiol 230(7):1580–1593. https://doi.org/10.1002/jcp.24905

Dunsmore SE, Saarialho-Kere UK, Roby JD, Wilson CL, Matrisian LM, Welgus HG, Parks WC (1998) Matrilysin expression and function in airway epithelium. J Clin Investig 102(7):1321–1331. https://doi.org/10.1172/JCI1516

Fang F, Luo W, Yang M, Yang P, Yang X (2019) Urinary matrix metalloproteinase-7 and prediction of AKI progression post cardiac surgery. Dis Mark 2019:9217571. https://doi.org/10.1155/2019/9217571

Farquhar MG, Palade GE (1963) Junctional complexes in various epithelia. J Cell Biol 17(5):375–412. https://doi.org/10.1083/jcb.17.2.375

Fu H, Zhou D, Zhu H, Liao J, Lin L, Hong X, Hou FF, Liu Y (2019) Matrix metalloproteinase-7 protects against acute kidney injury by priming renal tubules for survival and regeneration. Kidney Int 95(5):1167–1180. https://doi.org/10.1016/j.kint.2018.11.043

Furuse M, Tsukita S (2006) Claudins in occluding junctions of humans and flies. Trends in Cell Biol 16(4):181–188. https://doi.org/10.1016/j.tcb.2006.02.006

Gewin LS (2018) Renal tubule repair: is Wnt/β-catenin a friend or foe? Genes 9(2):58. https://doi.org/10.3390/genes9020058

Goligorsky MS, Lieberthal W, Racusen L, Simon EE (1993) Integrin receptors in renal tubular epithelium: new insights into pathophysiology of acute renal failure. Am J Physiol 264(1 Pt 2):F1–8. https://doi.org/10.1152/ajprenal.1993.264.1.F1

Ho J, Rush DN, Krokhin O, Antonovici M, Gao A, Bestland J, Wiebe C et al (2016) Elevated urinary matrix metalloproteinase-7 detects underlying renal allograft inflammation and injury. Transplantation 100(3):648–654. https://doi.org/10.1097/TP.0000000000000867

Ke B, Fan C, Yang L, Fang X (2017) Matrix metalloproteinases-7 and kidney fibrosis. Front Physiol 8:21. https://doi.org/10.3389/fphys.2017.00021

Kwon O, Nelson WJ, Sibley R, Huie P, Scandling JD, Dafoe D, Alfrey E, Myers BD (1998) Backleak, tight junctions, and cell-cell adhesion in postischemic injury to the renal allograft. J Clin Investig 101(10):2054–2064. https://doi.org/10.1172/JCI772

Manole E, Ceafalan LC, Oproiu AM, Popa-Wagner A, Popescu BO (2015) Claudin-1 and occludin expression in demyelinating peripheral neuropathies. Rom J Morphol Embryol 56(3):1097–1102

McGuire JK, Li Q, Parks WC (2003) Matrilysin (matrix metalloproteinase-7) mediates E-cadherin ectodomain shedding in injured lung epithelium. Am J Pathol 162(6):1831–1843. https://doi.org/10.1016/S0002-9440(10)64318-0

Parks WC, Wilson CL, López-Boado YS (2004) Matrix metalloproteinases as modulators of inflammation and innate immunity. Nat Rev Immunol 4(8):617–629. https://doi.org/10.1038/nri1418

Ponticelli C (2014) Ischaemia-reperfusion injury: a major protagonist in kidney transplantation. Nephrol Dialy Transplant 29(6):1134–1140. https://doi.org/10.1093/ndt/gft488

Prozialeck WC, Edwards JR (2007) Cell adhesion molecules in chemically-induced renal injury. Pharmacol Ther 114(1):74–93. https://doi.org/10.1016/j.pharmthera.2007.01.001

Racusen LC, Solez K (1991) Ideas in pathology. Exfoliation of renal tubular cells. Mod Pathol 4(3):368–370

Saat TC, van den Akker EK, Izermans JN, Dor FJ, de Bruin RW (2016) Improving the outcome of kidney transplantation by ameliorating renal ischemia reperfusion injury: lost in translation? J Transl Med 14(1):20. https://doi.org/10.1186/s12967-016-0767-2

Shirahata T, Nakamura H, Nakajima T, Nakamura M, Chubachi S, Yoshida S, Tsuduki K et al (2018) Plasma SE-cadherin and the plasma SE-cadherin/SVE-cadherin ratio are potential biomarkers for chronic obstructive pulmonary disease. Biomarkers 23(5):414–421. https://doi.org/10.1080/1354750X.2018.1434682

Smith SF, Hosgood SA, Nicholson ML (2019) Ischemia-reperfusion injury in renal transplantation: 3 key signaling pathways in tubular epithelial cells. Kidney Int 95(1):50–56. https://doi.org/10.1016/j.kint.2018.10.009

Tamura Y, Watanabe F, Nakatani T, Yasui K, Fuji M, Komurasaki T, Tsuzuki H et al (1998) Highly selective and orally active inhibitors of type IV collagenase (MMP-9 and MMP-2): N-sulfonylamino acid derivatives. J Med Chem 41(4):640–649. https://doi.org/10.1021/jm9707582

Tan RJ, Li Y, Rush BM, Cerqueira DM, Zhou D, Fu H, Ho J, Stolz DB, Liu Y (2019) Tubular injury triggers podocyte dysfunction by β-catenin–driven release of MMP-7. JCI Insight 4(24):e122399. https://doi.org/10.1172/jci.insight.122399

Tirapelli LF, Barione DF, Trazzi BFM, Tirapelli DPC, Novas PC, Silva CS, Martinez M et al (2009) Comparison of two models for evaluation histopathology of experimental renal ischemia. Transpl Proc 41(10):4083–4087. https://doi.org/10.1016/j.transproceed.2009.09.061

Wang D, Dai C, Li Y, Liu Y (2011) Canonical Wnt/β-catenin signaling mediates transforming growth factor-B1-driven podocyte injury and proteinuria. Kidney Int 80(11):1159–1169. https://doi.org/10.1038/ki.2011.255

Wang X, Miao Y, Ni J, Wang Y, Qian T, Yu J, Liu Q, Wang P, Yi S (2018) Peripheral nerve injury induces dynamic changes of tight junction components. Front Physiol 9:1519. https://doi.org/10.3389/fphys.2018.01519

Wu J, Zhao D, Wu S, Wang D (2015) Ang-(1–7) exerts protective role in blood-brain barrier damage by the balance of TIMP-1/MMP-9. Eur J Pharmacol 748:30–36. https://doi.org/10.1016/j.ejphar.2014.12.007

Yang X, Chen C, Teng S, Fu X, Zha Y, Liu H, Wang L et al (2017) Urinary matrix metalloproteinase-7 predicts severe AKI and poor outcomes after cardiac surgery. J Am Soc Nephrol: JASN 28(11):3373–3382. https://doi.org/10.1681/ASN.2017020142

Yang X, Ou J, Zhang H, Xu X, Zhu L, Li Q, Li J, Xie D, Sun J, Zha Y, Li Y (2019) Urinary matrix metalloproteinase 7 and prediction of IgA nephropathy progression'. Am J Kidney Dis. https://doi.org/10.1053/j.ajkd.2019.07.018

Yu AS, Alan SL (2015) Claudins and the kidney'. J Am Soc Nephrol 26(1):11–19. https://doi.org/10.1681/ASN.2014030284

Zhang S, An Q, Wang T, Gao S, Zhou G (2018) Autophagy- and MMP-2/9-mediated reduction and redistribution of ZO-1 contribute to

hyperglycemia-increased blood-brain barrier permeability during early reperfusion in stroke. Neuroscience 377:126–137. https://doi.org/10.1016/j.neuroscience.2018.02.035

Zhong Z, Hu Q, Fu Z, Wang R, Xiong Y, Zhang Y, Liu Z, Wang Y, Ye Q (2016) Increased expression of aldehyde dehydrogenase 2 reduces renal cell apoptosis during ischemia/reperfusion injury after hypothermic machine perfusion. Artif Organs 40(6):596–603. https://doi.org/10.1111/aor.12607

Zhou D, Tian Y, Sun L, Zhou L, Xiao L, Tan RJ, Tian J, Fu H, Hou FF, Liu Y (2017) Matrix metalloproteinase-7 is a urinary biomarker and pathogenic mediator of kidney fibrosis'. J Am Soc Nephrol: JASN 28(2):598–611. https://doi.org/10.1681/ASN.2016030354

Zhou X, Zang X, Guan Y, Tolbert T, Zhao TC, Bayliss G, Zhuang S (2018) Targeting enhancer of zeste homolog 2 protects against acute kidney injury. Cell Death Dise 9(11):1067. https://doi.org/10.1038/s41419-018-1012-0

Publisher's Note Springer Nature remains neutral with regard to jurisdictional claims in published maps and institutional affiliations.